

# Directional Flow Visualization of Vector Fields \*

Ed Boring and Alex Pang

Computer Science Department  
University of California, Santa Cruz, CA 95064  
edb@cse.ucsc.edu, pang@cse.ucsc.edu

## Abstract

This paper presents interactive flow visualization methods that highlight directional information in the flow field. An added benefit of the proposed methods is that they reduce the amount of data being displayed and hence reduce clutter. The main idea behind these methods is the use of light sources to select and highlight regions in the flow field with similar directions. Varying the lighting conditions, by moving the light source and/or adding more lights, emphasizes different vector directions, set of directions, and vectors within a specified angle of a particular direction. The methods are straight forward, computationally inexpensive, and can be combined with other techniques that use glyph representation and other flow geometry such as streamlines for feature visualization. We apply these methods to an analytic data set to help explain how they work, and then to a simulation data set to highlight flow reversals.

**Key Words and Phrases:** glyphs, streamlines, lighting, hue, value, region selection, clutter reduction, flow reversal.

## 1 INTRODUCTION

A vector field is rich in information. Each point in space represents a three-dimensional vector quantity having both *magnitude* and *direction*. Additionally, the field exhibits many derivable features such as *torsion*, *curvature*, *shear*, *acceleration*, and *convergence*. The difficulty is that there is no single natural way of visualizing entire 3D vector fields that highlights all these features [4]. As a result, numerous methods have been developed to visualize these different vector field properties.

In this paper we present a new vector visualization technique that emphasizes directional and magnitude information in the the vector field. Inspired by bump mapping techniques, methods using this technique treat the vector directions as some form of surface normals in the flow field. Variations on these normals are then used to shade feature glyphs inserted into the field. Vector information is visualized by adjusting glyph hue and intensity according to vector magnitude, vector direction, and lighting conditions. In particular, at each sampled point in the 3D volume, a glyph is associated with the vector at that point. Vector magnitude is mapped to glyph hue and and vector direction interacts with lighting conditions to determine the intensity of the glyph. Alternatively, vector magnitude can be mapped to glyph intensity and vector direction interacts with lighting conditions to determine the glyph hue.

Our approach is similar to Johannsen and Moorhead [5] where vector direction is mapped to hues in a color wheel, but extends the work to 3D vector fields and also add the ability to ability to refine directional search. Unlike Dovey's [3] work in vector plots of irregular grids, clutter reduction is achieved by displaying only the relevant vector glyphs instead of resampling and repositioning vector glyphs for the entire field. Our approach is also applicable to other means of displaying flow information such as streamlines.

In such cases, the interaction of the vector directions and lighting conditions are again used to determine how the geometry is to be rendered. This approach is much simpler and faster than the strategy proposed in [1] on rendering curves in 3-space.

There are several applications that motivate the need for methods that highlight regions of similar flow directions. Two of those that we worked with and will present in section 4 are: identifying the presence and locations of onshore or offshore flows in weather patterns (e.g. locations of northwesterly flows [2]); and identifying presence and locations of flow reversals from free stream flow in CFD simulations. Both of these can be easily highlighted with the methods described here.

## 2 DIRECTIONAL FLOW METHODS

In this research, we extend the bump mapped vector techniques [6] for identifying directional flow in 2D fields to three dimensions. Those techniques actually work with a 2-manifold surface – either a 2D planar cross section of a 3D flow field, or a surface in 3D. With surfaces, vector directions can be used to replace the surface normal, or alternatively used to alter the surface normal. Vector magnitudes are used in pseudocoloring the surface. Interactions of the perturbed surface normal and lighting conditions is then used to alter the pseudocoloring of the surface such that regions with similar flow directions (e.g. away from light source) are either dimmed or highlighted.

A direct extension of this idea to 3D vector volumes is possible but was not pursued due to the importance placed on interactivity. One direct extension would mean mapping cell densities to vector magnitudes, and cell opacities to the interaction of lighting conditions and altered cell normals, and then volume rendering the data. In addition to the loss of interactivity, the rendered image does not look as promising in presenting the regions of similar flow directions. Hence, we decided to apply the vector direction controlled shading to intermediate flow geometries such as glyphs and streamlines.

### Shading Cues from Vector Field

There are several ways of deriving shading cues from vector fields (e.g. [6]). Since we will mostly be using simple 1-manifold geometry (i.e. hedgehog lines and streamlines), and the lack of a natural surface normals for these shapes, we decided to use a straight replacement of the surface normal with the vector direction. That is,  $N' = V$ , where  $N'$  is the new surface normal, and  $V$  is the unit vector with the same direction as the vector flow at that point. Note that if a natural surface normal exists (e.g. spherical glyphs, etc.), then alternate mappings exist (e.g.  $N' = N + V$ ). The impact of these mappings becomes apparent when the vector field is viewed together with a moving light source. That is, the illumination of the vector field will be attenuated depending on the flow direction relative to the light source. Flow regions in the direction of the light source will be illuminated, while those in the opposite direction will

\*<http://www.cse.ucsc.edu/research/slv/3dbump.html>

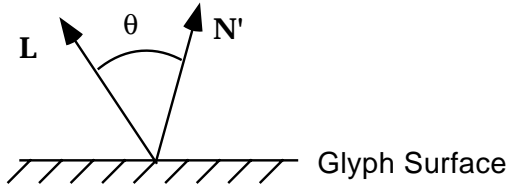


Figure 1: Illumination Model

be dark. A complementary effect can also be achieved if the vectors were negated (i.e.  $\mathbf{N}' = -\mathbf{V}$ ).

### Illumination Model

An illumination model is required in order to illuminate glyphs based on the derived surface normals and the lighting conditions. For this purpose, we use the Lambertian (diffuse) reflection model. In this model, the intensity of light reflected from a surface is a function of the angular distance,  $\theta$ , between the surface normal and the direction to the light source. Figure 1 illustrates the situation where a derived surface normal is illuminated from a light source in the direction  $\mathbf{L}$ . Using Lambertian reflection, the intensity of the light reflected from the glyph surface is given by:

$$I = I_\lambda k_d (\mathbf{L} \cdot \mathbf{N}') = I_\lambda k_d \cos(\theta) \quad (1)$$

where  $I$  is the computed intensity,  $k_d$  is the diffuse reflection coefficient,  $I_\lambda$  is the intensity of light source  $\lambda$ ,  $\mathbf{L}$  is a unit vector in the direction of the light, and  $\mathbf{N}$  is the unit surface normal.

### Mapping Vector Direction and Magnitude

There are several ways of mapping vector information to different color space. Two that look promising are: *direction-to-value illumination* and *direction-to-hue illumination*. The first maps vector direction to HSV value, and vector magnitude to HSV hue. The goal is to achieve a similar effect as the bump mapped vector fields – vectors pointing away from the light source will appear dimmer. The second maps vector direction to HSV hue, and vector magnitude to HSV value. It is different from standard direction-to-hue mapping in that the entire hue range is mapped to a smaller range of degrees allowing for better ability to distinguish among small angular differences.

#### 2.1 Direction-to-value Illumination

This method assigns an HSV hue based on vector magnitude and an HSV value based on vector direction. The HSV hue maps vector magnitude according to the following equation:

$$\mathcal{H} = \mathcal{H}_{min} + V_{sc}(\mathcal{H}_{max} - \mathcal{H}_{min}) \quad (2)$$

$$V_{sc} = \begin{cases} 0 & \text{if } V_s < 0 \\ 1 & \text{if } V_s > 1 \\ V_s & \text{otherwise} \end{cases}$$

$$V_s = \frac{\|\mathbf{V}\| - V_{min}}{V_{max} - V_{min}}$$

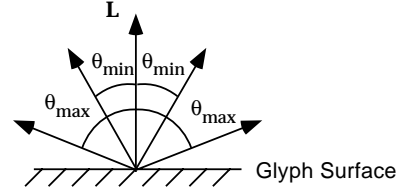


Figure 2: Range of Illumination Focus

$V_{sc}$  is the vector magnitude, scaled and clamped between 0 and 1 over the range  $V_{min}$  to  $V_{max}$ .  $V_{min}$  and  $V_{max}$  are chosen to scale the visualization to a vector magnitude range of interest. Vectors with magnitudes outside the range are clamped or maybe filtered if desired.  $\mathcal{H}_{min}$  and  $\mathcal{H}_{max}$  are the HSV hue ranges used in the mapping. The smallest scaled and clamped vector magnitude maps to  $\mathcal{H}_{min}$  and the largest maps to  $\mathcal{H}_{max}$ .

As a typical example, we want to visualize the vectors over the entire vector magnitude range 0 to  $V'_{max}$  where  $V'_{max}$  is the maximum magnitude vector in the entire field. A hue mapping is chosen so that 0 magnitude vectors map to  $\mathcal{H}_{min} = 300$  (magenta) and maximum magnitude vectors map to  $\mathcal{H}_{max} = 0$  (red). Equation 2 then reduces to:

$$\mathcal{H} = 300 - 300 \frac{\|\mathbf{V}\|}{V'_{max}}$$

A direction to value mapping based on the illumination conditions and the derived surface normals is required. A modification to the Lambertian illumination (equation 1) provides the direction-to-value mapping equation:

$$\mathcal{V} = \mathcal{V}_{min} + \cos(\theta_{sc})(\mathcal{V}_{max} - \mathcal{V}_{min}) \quad (3)$$

$$\theta_{sc} = \begin{cases} 0 & \text{if } \theta_s < 0 \\ 90 & \text{if } \theta_s > 90 \\ \theta_s & \text{otherwise} \end{cases}$$

$$\theta_s = 90 \frac{\theta - \theta_{min}}{\theta_{max} - \theta_{min}}$$

$$\theta = \arccos(\mathbf{L} \cdot \mathbf{N}')$$

$\theta_{sc}$  is the angle between the light and the normal, scaled and clamped on the range  $\theta_{min}$  to  $\theta_{max}$ . The angular distance  $\theta$  between the normal and light direction is first scaled and clamped between 0 and 1 over  $\theta_{min}$  to  $\theta_{max}$ . It is then scaled by 90 degrees to allow for full cosine attenuation in this range. Figure 2 illustrates these angular ranges.  $\theta_{min}$  and  $\theta_{max}$  are chosen to provide *illumination focus*. That is, glyphs with vector directions lying in a specified angular range of the light direction are illuminated, thus focusing the visualization on regions with flows with the specified directional range.

$\mathcal{V}_{min}$  and  $\mathcal{V}_{max}$  specify the HSV value range used in the mapping. The smallest, scaled, and clamped angle ( $\theta_{sc} = 0$ ) maps to  $\mathcal{V}_{max}$  and the largest ( $\theta_{sc} = 90$ ) to  $\mathcal{V}_{min}$ .

As a typical illumination example, we want to visualize glyphs with bumped mapped normals whose angular distance from the light lie between  $\theta_{min} = 0$  and  $\theta_{max} = 90$  degrees. HSV value range is chosen so that the angular distance of  $\theta = 0$  degrees maps to a value of  $\mathcal{V}_{max} = 1$  and the angular distance of  $\theta = 90$  degrees maps to a value of  $\mathcal{V}_{min} = 0$ . Equation 3 reduces to:

$$\mathcal{V} = \cos(\theta) = \mathbf{L} \cdot \mathbf{N}'$$

## 2.2 Direction-to-hue Illumination

Direction-to-hue illumination exchanges the role of HSV hue and HSV value used in direction-to-value illumination. Here, HSV value is assigned using the magnitude-to-value mapping equation:

$$\mathcal{V} = \mathcal{V}_{min} + V_{sc}(\mathcal{V}_{max} - \mathcal{V}_{min}) \quad (4)$$

where  $V_{sc}$  is given in equation 2.

For example, we want to visualize the vectors over the entire vector magnitude range 0 to  $V'_{max}$  where  $V'_{max}$  is the maximum magnitude vector in the entire field. HSV value mapping is chosen so that 0 magnitude vectors map to  $\mathcal{V}_{min} = 0$  and maximum magnitude vectors map to  $\mathcal{V}_{max} = 1$ . Equation 4 then reduces to:

$$\mathcal{V} = \frac{\|\mathbf{V}\|}{V'_{max}}$$

HSV hue is assigned using the direction-to-hue mapping equation:

$$\mathcal{H} = \mathcal{H}_{min} + \cos(\theta_{sc})(\mathcal{H}_{max} - \mathcal{H}_{min}) \quad (5)$$

where  $\theta_{sc}$  is the same given in equation 3.

As an illumination example, assume we want to visualize glyphs with normals whose angular distances from the light lie between  $\theta = 0$  and 90 degrees. HSV hue range is chosen so that an angular distance of  $\theta = 0$  degrees maps to a HSV hue of  $\mathcal{H}_{max} = 0$  (red) and an angular distance of  $\theta = 90$  degrees maps to a HSV hue of  $\mathcal{H}_{min} = 300$  (magenta). Equation 3 reduces to:

$$\mathcal{H} = 300 - 300 \cos(\theta)$$

## 3 IMPLEMENTATION

We implemented our flow visualization techniques using the Visualization Toolkit (VTK) [8]. VTK is an object-oriented 3-D graphics library that implements many common visualization methods. VTK provided our main visualization pipeline and many of the methods we used for verifying our techniques including file reading, grid handling, isosurface, streamline, and hedgehog visualization tools. To this core library we added methods for producing scalar fields from the illumination equations, and routines for HSV color space mapping, grid filtering, and isosurface generation based on these fields. The VTK streamlines used in our visualizations are constructed using second order Runge-Kutta method. All grids and data sets are original with no resampling.

## 4 RESULTS

We tested the 3D directional flow visualization methods on 3 different types of data: (a) analytical data set with simple helical flow to help understand and demonstrate how the method works, (b) meteorological wind data of the Monterey Bay area provided through the REINAS project [7], and (c) the Delta wing at 40 degree angle of attack CFD data set (<http://chuck.nas.nasa.gov/DataSets/Ekaterinaris.1/index.html>) to illustrate flow reversals. Both hedgehog lines and streamlines were used in these data sets. In addition, isosurfaces of  $\cos(\theta_{sc}) = 0$  (indicating angular relationship between light source and vector

directions) were constructed to verify the methods. Finally, hedgehog lines are automatically removed when the direction falls outside of the illumination focus or magnitude falls below some threshold value. This additional culling helps improve the overall presentation by removing what would otherwise be dark, uninteresting, and possibly occluding geometry. This threshold parameter is user definable. For the images, geometry is not drawn if  $\cos(\theta_{sc}) = 0$  or if  $V_{sc} = 0$ .

Color plates 1 to 6 show some examples of applying the directional flow visualization techniques to 3D vector fields. In each visualization, the volume is populated with fixed length hedgehog lines aligned with the local vector direction. The direction of an infinite light source is indicated by an arrow visible in each color plate. For direction-to-hue mappings, red maps to an angle of 0 degrees between light and vector direction (i.e. vector direction is opposite of light direction), while magenta maps to the maximum angle defined by the illumination focus. For direction-to-value mapping, red maps to maximum vector magnitude, while magenta maps to minimum vector magnitude.

Color plates 1 and 2 are visualizations of an analytical helical flow described by:  $\mathbf{v}(x, y, z) = -by\mathbf{i} + bx\mathbf{j} + ck$ , where  $b$  and  $c$  are constants and affect the pitch of the helix. The flow is in a counter-clockwise direction as viewed from color plates 1 and 2, with a single light source coming from the left. The bottom halves of the data sets are not visible as they are culled from the presentation because the velocity field there does not have any components towards the light source. Only the top half of the helical flows are visible since this is the only region where the flow has any component towards the light source. More generally, only those flow regions whose vector direction lie within the illumination focus will be visible.

Visualizations of this analytical data set serve two purposes: to help us validate our technique, and to help demonstrate how it works on a simple and well understood data set. In color plate 1, hue is mapped to vector direction. Here, one can observe the symmetric distribution of hue as the angle between the light source and vector directions range from -90 to 0 to 90. This also illustrates why the bottom half of the data set is not visible. Dot products of the light vector and vector direction are being taken, and since the bottom half have flow components that are all away from the light source, they are all culled out. One can also observe that the hedgehog lines appear dimmer (indicating a lower magnitude) at the center of the flow, and brighter near the edge of the data set.

In color plate 2, hue is mapped to vector magnitude. Here, one can observe the hue changing from magenta to red as one goes out of the center. That is, the vector magnitude increases as one moves away from the center and go towards the edge. This illustrates an alternative mapping which seem to work better at distinguishing vector magnitudes compared to the hue-to-value mapping used in color plate 1. Another thing that one can observe in color plate 2 is a higher intensity (value) for the hedgehog lines near the vertical ( $y$ ) axis. This is accounted for by the fact that the directions of the vectors around the vertical axis are more closely lined up with the light source than those further away.

Color plates 3 and 4 illustrate the same method applied to meteorological data. Color plate 3 applies direction-to-hue illumination while color plate 4 uses the direction-to-value mapping. An illumination focus of 0 to 30 degrees is applied in both cases. These images indicate the regions of the flow volume whose flow directions have components towards the light source. Semi-transparent isosurfaces are constructed on the threshold  $\cos(\theta_{sc}) = 0$ . Thus, the isosurfaces bound all the volumes where the vectors within the volume lie within the maximum angular extents of the illumination focus. In this case the isosurfaces bound volumes where the vector directions all lie within 30 degrees of the light vector. In color plate 3 (direction-to-hue mapping) it can be observed that the flow direc-

tion in each region are most closely aligned with the light source near the region centers. That is, there are more red hedgehog lines near the region centers and more magenta lines on the periphery of these regions. In color plate 4 (direction-to-value mapping), with hue indicating magnitude of the flow, one can observe that flow magnitudes are generally not very strong around the isosurfaces. When isosurfaces are removed, one can also observe that lines near the region centers are more intense than those on the periphery. The isosurfaces, while not necessary for these illustrations and may at times occlude some regions of interest, also helped in the validation of our methods. Hence, they were provided with the ability of turning them on or off.

Color plates 5 and 6 show the technique applied to a CFD solution for a delta wing at a 40 degree angle of attack. Both figures use direction-to-value mapping with an illumination focus of 0 to 90 degrees. To prove that our technique is superior in identifying regions of similar flow directions, we use these two color plates regions of flow reversals. Flow reversals are regions in the flow field where the flow direction is opposite the free stream flow. Hence, to identify these flow reversals, we simply set the illumination direction in the same direction as the free stream flow of 40 degrees. Of the more than 200,000 grid points in the data set, only 2 distinct regions showed signs of flow reversals: one region is on the edge of the wing, very near the surface; the second region is within a vortex core above the wing.

Color plate 5 zooms in on the field reversal phenomena. Two distinct regions of hedgehog lines can be seen: one set near the wing's edge, the other approximately above it. Streamlines were seeded near the nose of the delta wing. Those rising above the wing illustrate the flow reversal within the core, which also wraps around the second set of hedgehog lines. However, with the streamlines alone, it was very difficult to find the seed points that would show the first flow reversal region. This first region is made up of hedgehog lines near the edge of the wing which look like fans, with each fan originating from a single point. In fact, each vector in the fan originates from a different grid cell. They are just tightly stacked in the z direction.

Color plate 6 uses isosurfaces of  $\cos(\theta_{sc}) = 0$  to identify the envelope of these two flow reversal regions. Hedgehog lines are removed at this point to reduce display clutter. Note that hedgehog lines are simply visual manifestations of the directional flow algorithm – the isosurfaces can be viewed as an alternate form of presenting the region of interest. In this color plate, there are again two areas of field reversals visible. The first, well above the wing and stretching behind the wing, is a field reversal associated with a vortex core. The extent of this core region is enclosed by the larger isosurface. This observation is confirmed by streamlines generated at the nose of the wing. Note that two of the streamlines spiral around the vortex core region while one of the streamlines enters the core and reverses direction. The second field reversal is located just above the surface near the edge and rear portion of the wing. This particular reversal is difficult to find using streamline techniques alone. Our attempt to find appropriate seed points to visualize this particular reversal using interactive positioning of a seed rake was time consuming but identification using the directional flow technique was immediate and straightforward.

## 5 CONCLUSIONS

3D vector fields in combination with either a direction-to-value or direction-to-hue illumination model form a natural paradigm for directional flow field visualization. It is an inexpensive technique. The real power comes from the realtime interaction with the lighting conditions to highlight regions of different flow directions. Regions containing vectors aligned in the light direction appear as clusters or clouds which change shape and location as the lighting

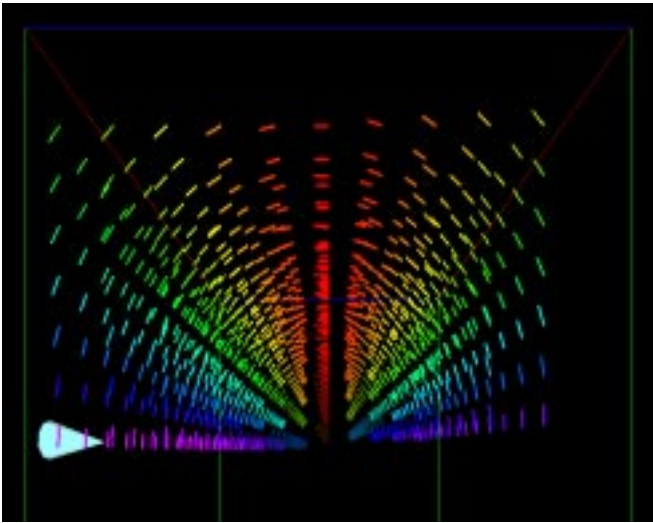
conditions evolve. The ability to either add multiple lights or adjust mapping parameters to narrow the focus of the flow directions help users understand the flow pattern of the 3D flow field. After some initial training to get used to the interpretation of the direction-to-hue and the direction-to-value mappings, one can easily reveal and understand flow details. Application of these methods can also partially reduce the cluttering problem by rendering only those vectors in the field that are under illumination from the current lighting direction and illumination focus.

## ACKNOWLEDGEMENTS

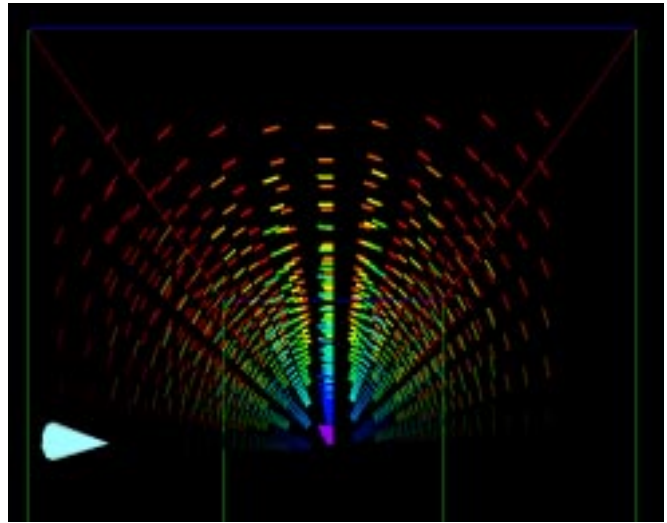
We would like to thank Naim Alper for his contribution to the work on 2D bump mapped vector fields, Wendell Nuss for his NORAPS meteorology data sets, and David Kenwright and David Lane for discussions on flow reversals. We would also like to thank the Santa Cruz Laboratory for Visualization and Graphics (SLVG) for the wonderful research environment. This project is supported by ONR grant N00014-92-J-1807, NASA Cooperative Agreement NCC2-5176, and NSF grant IRI-9423881.

## References

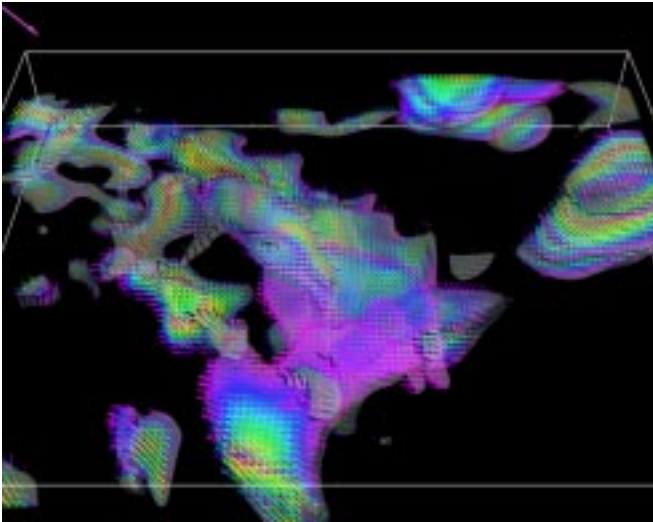
- [1] David C. Banks. Illumination in diverse codimensions. *Computer Graphics (ACM SIGGRAPH Proceedings)*, pages 327–334, July 1994.
- [2] A.F.C. Bridger, A.J. Becker, F.L. Ludwig, and R.M. Endlich. Evaluation of the WOCSS wind analysis scheme for the San Francisco Bay Area. *Journal of Applied Meteorology*, 33(10):1210 – 1218, October 1994.
- [3] Don Dovey. Vector plots for irregular grids. In *Proceedings: Visualization '95*, pages 248 – 253. IEEE Computer Society, 1995.
- [4] L. Hesselink, F. Post, and J.J. van Wijk. Research issues in vector and tensor field visualization. *IEEE Computer Graphics and Applications*, 14(2):76–79, March 1994.
- [5] A. Johannsen and R. Moorhead II. AGP: ocean model flow visualization. *IEEE Computer Graphics and Applications*, 15(4):28–33, July 1995.
- [6] Alex Pang and Naim Alper. Bump mapped vector fields. In *SPIE & IS&T Conference Proceedings on Electronic Imaging, Vol. 2410: Visual Data Exploration and Analysis II*, pages 78–86, color plate page 205. SPIE, February 1995.
- [7] Alex Pang and Dan Fernandez. REINAS visualization and instrumentation. In *Proceedings of Oceans'95 Conference*, pages 1892–1899, October 1995.
- [8] Will Schroeder, Ken Martin, and Bill Lorensen. *The Visualization Toolkit: An Object-Oriented Approach to 3D Graphics*. Prentice Hall, New Jersey, 1996.



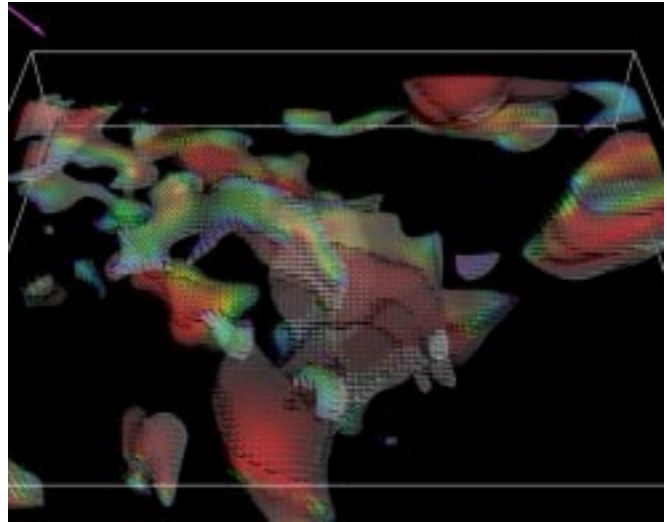
Color Plate 1: Direction-hue, helix data.



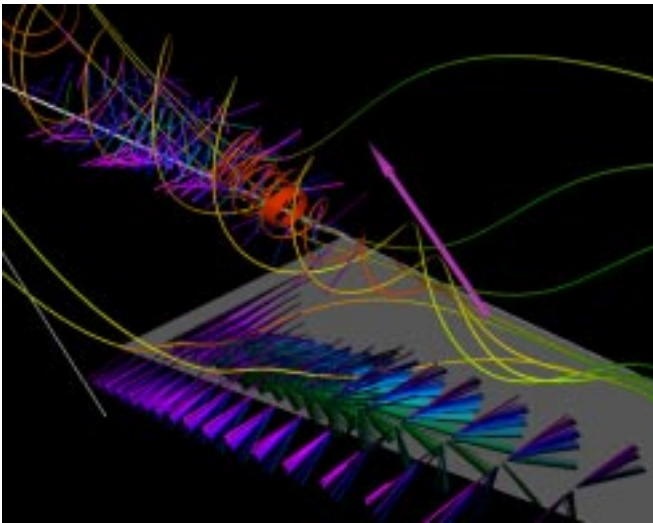
Color Plate 2: Direction-value, helix data.



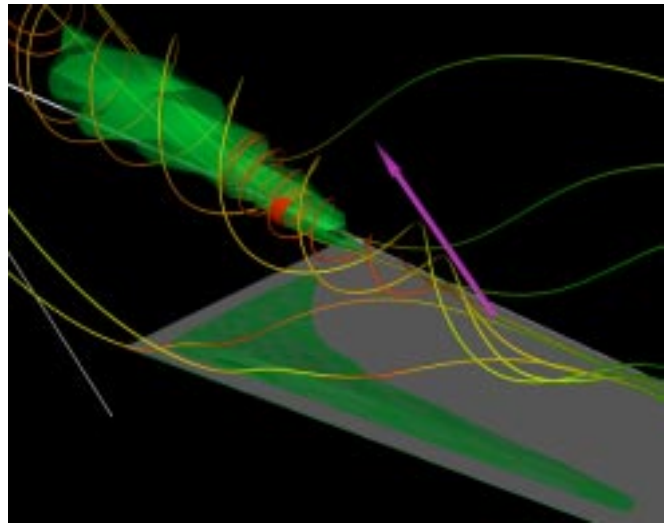
Color Plate 3: Direction-hue, weather data.



Color Plate 4: Direction-value, weather data.



Color Plate 5: Direction-value, delta wing.



Color Plate 6: Direction-value, delta wing.